ELSEVIER

Contents lists available at ScienceDirect

Dendrochronologia

journal homepage: www.elsevier.com/locate/dendro



Check for updates

Dendroanatomy of xylem hydraulics in two pine species: Efficiency prevails on safety for basal area growth in drought-prone conditions

Emanuele Ziaco^{a,*}, Xinsheng Liu^b, Franco Biondi^c

- ^a Department of Geography, Johannes Gutenberg University, Mainz, Germany
- ^b School of Geography and Tourism, Anhui Normal University, Wuhu, China
- ^c DendroLab, Department of Natural Resources and Environmental Science, University of Nevada, Reno, United States

ARTICLE INFO

Keywords: Basal area increment Bristlecone pine Hydraulic efficiency Limber pine NevCAN Quantitative wood anatomy

ABSTRACT

Xylem structure optimizes water conductivity while preventing hydraulic failure via embolism resistance, but how this process is modulated by climate variability and how it affects secondary growth in mature trees is still not fully understood, particularly in water-limited environments. Using quantitative wood anatomy techniques, we estimated xylem anatomical proxies for hydraulic efficiency (xylem specific conductivity, Ks) and safety (cell wall reinforcement, wrein) in two western US conifers, Pinus flexilis and Pinus longaeva, at a montane and subalpine location respectively. We built two large datasets (570 rings for P. flexilis, 635 rings for P. longaeva) to investigate 1) the variability of anatomical parameters (i.e lumen diameter, cell wall thickness) and hydraulic proxies along the stem in the five outermost rings (2009-2013); 2) the response of hydraulic proxies to daily climate over a period of 24 years (1990-2013); and 3) the relationship between xylem hydraulic architecture and basal area increment (BAI). Lumen diameter scaled along the stem following a power function, but the scaling patterns of cell wall thickness and hydraulic proxies differed significantly between species. From 1990–2013, Ks decreased in both species, whereas wrein increased only in P. longaeva, while no trends were observed in BAI. Climate sensitivity of Ks peaked over a longer period (84-102 days) compared to wrein (20-55 days), responding to increasing minimum temperature. In both species, Ks was a better predictor of BAI than wrein, indicating that, even under severely water-limited conditions, radial growth is linked to hydraulic efficiency rather than safety. Based on the variability of cell density along the stem, the trade-off between hydraulic efficiency and safety in P. longaeva appeared to be controlled by a strategy of space occupation. Characterizing the mechanistic relationship between xylem anatomy, plant hydraulic functioning, and stem growth is necessary to better understand climate-growth relationships in the western US and species' growth plasticity under future climate change scenarios.

1. Introduction

The anatomical structure of wood represents the tree hydraulic architecture, which balances trunk capacity to effectively transport water from the roots to the canopy against the risk of xylem implosion (Cruiziat et al., 2002; Mencuccini et al., 1997; Tyree and Zimmermann, 2002). During xylem formation, wood cellular features, such as the size of tracheid lumens and walls, vary in response to external factors (Buttò et al., 2019; Cabon et al., 2020a; Cuny et al., 2014; Zheng et al., 2022). As xylem anatomy changes inter- and intra-annually in response to internal and external factors, so does stem hydraulic architecture (Bryukhanova and Fonti, 2013; Deslauriers et al., 2017; Hudson et al., 2018),

ultimately affecting tree performance under a broad range of climatic and environmental conditions (Gleason et al., 2016; Lourenço et al., 2022; McCulloh et al., 2014; Sasani et al., 2021).

Two processes, namely the optimization of water transport ("efficiency") and prevention of hydraulic failure ("safety"), represent one of the main mechanistic linkages between xylem cellular structure and plant secondary growth (Anderegg et al., 2016; Pacheco et al., 2015; Pfautsch, 2016). On the one hand, hydraulic traits linked to xylem conduits properties reflect the tree hydration status during cell formation and modulate stem-water dynamics (Hudson et al., 2018; Pellizzari et al., 2016; Prendin et al., 2018). In fact, the theoretical amount of water flowing through the stem can be calculated from conduit size

E-mail address: eziaco@uni-mainz.de (E. Ziaco).

^{*} Corresponding author.

according to the Hagen-Poiseuille law (Tyree and Zimmermann, 2002), while the thickness of cellular walls relative to conduit size can predict xylem resistance to implosion under highly negative pressures (Hacke et al., 2001), such as those experienced during drought or freezing events (Zheng et al., 2022). Tree secondary growth, on the other hand, can be quantified using basal area increment, which is equivalent to tree-ring area (Biondi and Qeadan, 2008), and is an index of the amount of new wood formed every year throughout the growing season (Vospernik, 2021).

In theory, higher growth rates should be associated with more efficient xylem, while under severely constraining environmental conditions, with reduced radial growth, hydraulically safer xylem should be observed (Anderegg et al., 2016; Pfautsch, 2016). Anatomical traits favoring xylem efficiency (i.e. tracheids lumen area) and those promoting xylem safety (i.e cell wall thickness) generally show respectively a positive and negative correlation with plant secondary growth (Hoeber et al., 2014; Poorter et al., 2010). Higher growth rates are associated with increased conductivity in woody species from temperate (Gleason et al., 2018; Russo et al., 2010) and tropical environments (Fan et al., 2012). However, a weak correlation was found between xylem specific conductivity and growth in the branches of several broadleaf and conifer species in Mediterranean regions (Rosas et al., 2021; Sterck et al., 2012). If wood anatomy-growth relationships are investigated at the branch level (Prendin et al., 2018; Sterck et al., 2012), rather than on the main stem (Domec and Gartner, 2003; Islam et al., 2019; Piermattei et al., 2020), dendrochronological measurements cannot usually be employed to define long term trait-growth relationships (Zimmermann et al., 2021).

Xylem functional traits derived from quantitative wood anatomy (von Arx et al., 2016) have been used for retrospective analysis of species responses to climatic variability because of their sensitivity to environmental conditions and their persistence in the wood of living and dead trees for several decades (Castagneri et al., 2017; Puchi et al., 2021). As anthropogenic forcing is predicted to increase the frequency and severity of extreme climatic events (Cook et al., 2020; Stevenson et al., 2022), assessing how inter-annual variability of xylem hydraulic architecture determines plant physiological responses helps with evaluating species plasticity to past and possibly future hydroclimatic conditions (Anderegg and Meinzer, 2015). However, a detailed characterization of such xylem hydraulic adjustments has to account for the variability of wood anatomical parameters, in particular the widening of conduits (i.e. tracheids) from the top to the bottom of the stem (Olson et al., 2021; Olson et al., 2018; Soriano et al., 2020). The distance from the stem apex (hereinafter called "stem length") influences wood anatomical parameters, and conduit size widens with increasing stem length following a power function with an ~0.2 exponential scaling factor (Anfodillo et al., 2006). Hence, comparing species and/or individuals with different height should consider the vertical variability of wood anatomical structures, particularly when assessing the relationships between xylem cellular features and plant water dynamics (De Micco et al., 2008).

Plant hydraulic functioning under controlled conditions is relatively well understood (Cochard et al., 2021; Pfautsch, 2016), but studies of tree hydraulic adjustments that modulate secondary growth, particularly under natural conditions, are less common (Chenlemuge et al., 2015; Khansaritoreh et al., 2018; Zimmermann et al., 2021). Since droughts are expected to become globally more frequent (Cook et al., 2020), assessing the relationship between xylem hydraulic functioning and tree growth in arid environments can provide valuable information to understand plants' plasticity under water-limited conditions (Berkelhammer et al., 2020; Férriz et al., 2023). The Great Basin of North America represents the largest arid region of the United States, characterized by extreme dryness, particularly in Nevada (Grayson, 2011), making it suitable to investigate anatomy-growth relationship and its response to changing environmental conditions. At high elevation, mountain ranges of the Great Basin are often dominated by limber pine

(*Pinus flexilis* E.James) and bristlecone pine (*Pinus longaeva* D. K. Bailey). Our own work has contributed to uncover species-specific responses to hydroclimatic variability in these ecosystems (Liu and Biondi, 2020; Liu et al., 2021; Ziaco and Biondi, 2016, 2018; Ziaco et al., 2016a). However, climate-growth relationships at or near the treeline remain notoriously complex for these species (Bunn et al., 2018; Salzer et al., 2014), interacting in multiple ways with demographic processes of these conifer populations (Millar et al., 2015).

In the present study, we tested the hypothesis that tree growth might be associated differently by species either to hydraulic safety or to hydraulic efficiency in response to varying environmental conditions, especially drought stress. We estimated xylem anatomical proxies for theoretical hydraulic efficiency and safety in two natural stands of P. flexilis and P. longaeva located in central-eastern Nevada (USA). We then applied dendroclimatic techniques to answer the following questions: 1) how is the variability of xylem hydraulic architecture related to that of wood anatomical parameters?; 2) what is the temporal window in which tree hydraulic functioning is more affected by climate?; 3) how can changes in hydraulic architecture determined by wood anatomy affect tree annual basal area increment? For these purposes, we characterized a) the variability of xylem anatomical and hydraulic traits along the stem in the 5 outermost functional rings over the period 2009–2013, and b) temporal changes in plant hydraulics over a period of 24 years (1990-2013).

2. Materials and methods

2.1. Study area

This study was conducted on two populations of Pinus flexilis (38°53'24" N, 114°19'53" W) and P. longaeva (38°54'22" N, 114°18'32" W) located in the Snake Range, eastern Nevada, USA (Fig. 1a) and included in NevCAN (Nevada Climate-ecohydrological Assessment Network; https://nevcan.dri.edu), an elevational transect of fullyautomated, instrumented stations established between 2011 and 2013 in the Great Basin (Mensing et al., 2013). The distribution of P. flexilis generally extends into lower elevations compared to that of P. longaeva, found at or near treeline (Lanner, 1984). At the upper limit of its altitudinal distribution, P. flexilis merges with P. longaeva. At our study area, Pinus flexilis dominates a mixed conifer stand at an elevation of 2810 m asl, in the montane belt of the Snake Range, while P. longaeva is dominant near treeline (3355 m asl), in the subalpine zone. Recent research in the Great Basin found that while the upper limits for both species have shifted upward since 1950, P. flexilis is using its broader range of tolerance during early-life stages to leap-frog over P. longaeva and regenerate at high elevations (Millar et al., 2015; Smithers et al., 2021; Smithers et al., 2018). Other conifer species, Abies concolor (Gordon & Glend.) Lindley ex Hildebrand and Pseudotsuga menziesii (Mirb.) Franco at the montane site, and Picea engelmannii Engelm. at the subalpine site, are also present.

According to NevCAN data, mean annual temperature at the montane site during the period 2011–2020 was 5.2 $^{\circ}\text{C}$ (mean maximum and minimum monthly temperature respectively 12.1 °C and 0.0 °C), with July (mean monthly temperature = 17.7 $^{\circ}$ C) and December (mean monthly temperature = -4.5 °C) being the warmest and coldest months, respectively. The subalpine site had mean annual temperature of 1.5 °C during the period 2011-2020, with mean annual maximum and minimum temperatures of 6.7 °C and - 2.8 °C. July was the warmest month (mean monthly temperature = 12.9 °C) and February (mean monthly temperature $= -7.3\,^{\circ}\text{C}$) the coldest one. Total annual precipitation averaged 390 mm at the montane site, mostly (40.1%) falling between March and May, and it increased to an average of 472 mm at the subalpine site, with May (13.9% of annual total rainfall) and April (12.5%) being the wettest months. Longer climatic records were obtained from the public-domain PRISM (Parameter-elevation Relationships on Independent Slopes Model) dataset (Daly et al., 2008) by selecting the two

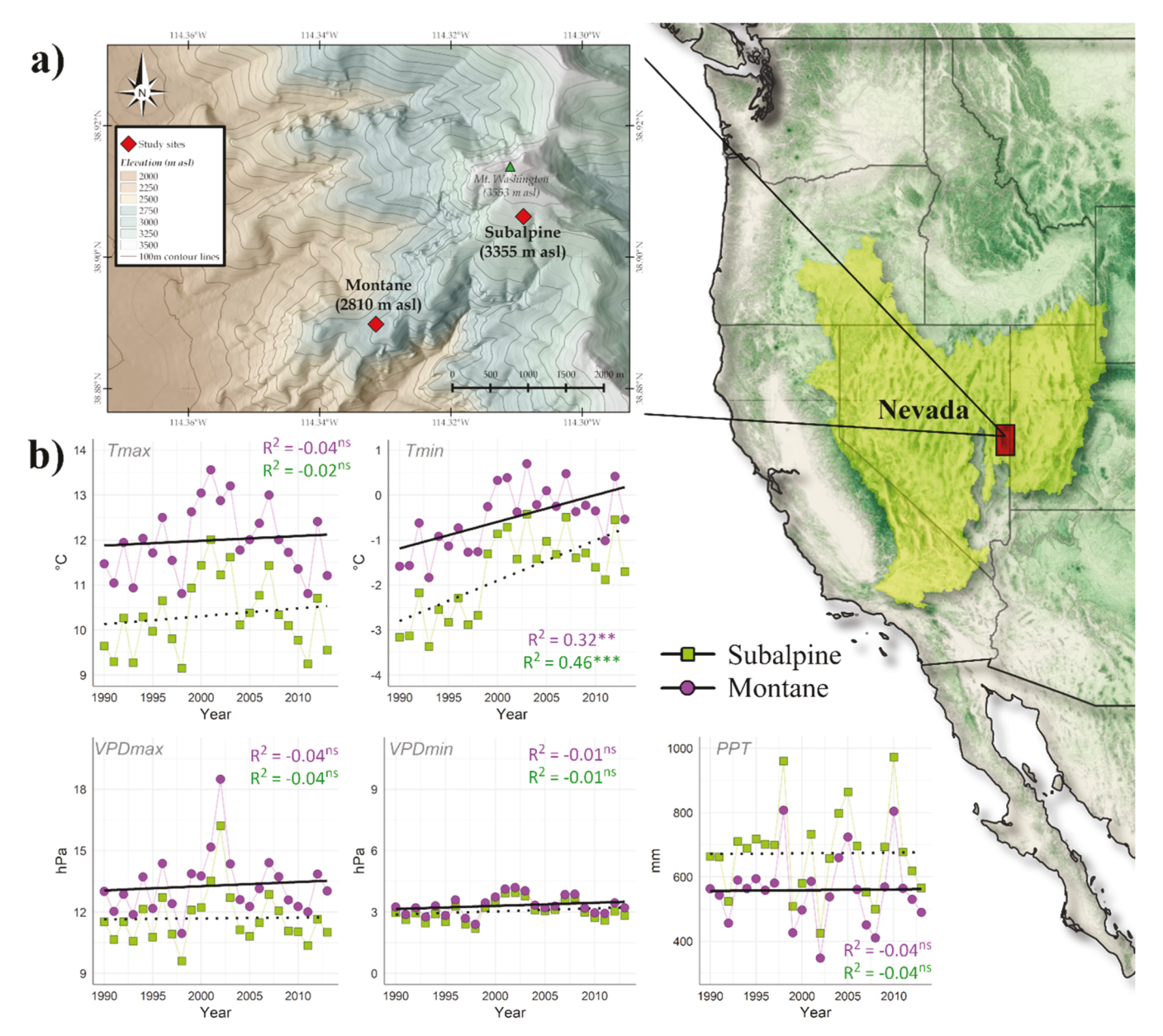


Fig. 1. a) Geographical location of the two study sites within the western north America and the Great Basin (yellow shaded area). The location of the Snake Range is highlighted by a red rectangle; b) time series and linear regressions for annual mean values of selected climatic parameters (maximum and minimum temperature, maximum and minimum vapor pressure deficit, and total precipitation) at the Subalpine and Montane sites for the period 1990–2013. R^2 and significance (*** p < 0.001; ** p < 0.001) are color coded.

4-km grid cells that include the montane and subalpine sites. Daily PRISM records of maximum (Tmax) and minimum (Tmin) air temperature, total precipitation (Ppt), maximum (VPDmax) and minimum (VPDmin) vapor pressure deficit covered the period 1981–2019.

2.2. Sample collection and preparation

In each stand, a total of 8 healthy individuals, showing no signs of crown or stem damage, were sampled in August 2014. Sampled trees were chosen among all diameter classes to represent the size distribution within each population. Average diameter at breast height (~1.3 m from the ground) of selected trees was 15 cm (range 9–24 cm) for *P. flexilis* and 36 cm (range 21–47 cm) for *P. longaeva*. Tree height for each tree was carefully measured using a clinometer from a linear distance of 20 m. *P. flexilis* had a mean height of 5.9 m (range 4.5–7.1 m), while the mean height of sampled *P. longaeva* was 9.7 m (range

6.9–11.8 m). Tree age was determined by collecting an increment core at breast height. Sampled *P. flexilis* trees were younger (mean of 64 ± 15 years) compared to *P. longaeva* ones (mean of 156 ± 31 years).

For each tree, microcores with a diameter of 2 mm and \sim 20 mm long were collected using a Trephor (Rossi et al., 2006a) every 50 cm along the stem, starting from the ground level up to the highest reachable point using a ladder. To quantify the scaling of wood anatomical parameters along the stem, the distance from the stem apex of each sampling point needs to be known (Carrer et al., 2015). Since a direct measurement of the distance from the treetop was impossible in the field, for each sampling point we calculated the difference between the total tree height and the distance from the ground, and then aggregated the microcores in 50-cm stem-length classes. In *P. flexilis* we were able to reach up to 2.25 m from the treetop, while the sampling in *P. longaeva* arrived at 3.75 m from the top. After collection, microcores were stored in 70% ethanol and placed in ice. The relatively short length of the

microcores ensured that we sampled only the sapwood (Liu and Biondi, 2020). However, given the slow growth rates at these sites, each microcore included several (i.e. up to 30) annual rings. A total of 108 microcores (53 for *P. flexilis* and 55 for *P. longaeva*) were collected, and at each sampling point along the stem the diameter was carefully recorded using a measuring tape.

In the lab, microcores were dehydrated in a tissue processor LEICA TP1020 with ethanol and a clearing agent (Protocol SAFECLEAR II) (Rossi et al., 2006a) and then embedded in paraffin blocks. Transversal sections, $10\text{--}12\,\mu\text{m}$ thick, were cut with a rotary microtome and mounted on microscope slides using PermountTM mounting medium. Paraffin was then removed through successive baths in SAFECLEAR II and ethanol 100%, and sections were finally stained with safranin (0.50% aqueous solution). Several highly contrasted black and white images at 100--200x magnification were captured with a Lumenera Infinity1 digital camera mounted on a Nikon Eclipse Ci-L microscope across the entire length of each section, and then merged in a single image using Adobe Photoshop©.

2.3. Basal area increment, anatomical measurement, and hydraulic parameters

Tree ring-widths and wood anatomical parameters were measured with the software WinCELL (Guay, 2013). Ring-widths were measured on each microcore, then visually and statistically crossdated against existing chronologies developed for *P. flexilis (unpublished data)* and *P. longaeva* (Ziaco et al., 2016a) at the two sites according to standard dendrochronological procedures (Stokes and Smiley, 1996). Annually resolved time series of Basal Area Increment (BAI, mm²), or ring area, were calculated for each microcore using crossdated ring-width as follows:

$$BAI_t = \frac{\pi}{4} \left[D_t^2 - \left(D_t - 2w_t \right)^2 \right]$$

where D_t is the stem diameter (in mm) at the end of the annual increment and w_t is the annual ring-width (in mm). BAI series were computed with the function bai.out() in the R package dplR (Bunn et al., 2014).

On each sample, anatomical parameters were measured for each tree ring by selecting an area covering the entire ring (i.e. earlywood and latewood) while avoiding resin ducts and cracks. Measured anatomical parameters included tracheid radial lumen diameter (LD, μm), and cell wall thickness (CWT, μm), defined as the average between radial wall thicknesses. For each ring, the cell density (Dens, N/mm²), defined as the number of cells by the area analyzed, was also measured. We pooled together earlywood and latewood since at these locations and for these two species, latewood is generally formed only by a few (i.e. 2–3) lines of cells (Ziaco and Biondi, 2016; Ziaco et al., 2016a) and the transition between earlywood and latewood is driven by the reduction in lumen radial diameter rather than by an increase in cell wall thickness in the latter part of the ring (Carvalho et al., 2015), with little effect on whole ring hydraulic efficiency and/or safety.

Hydraulic efficiency of the stem was represented by xylem specific conductivity Ks, i.e. the theoretical amount of water flowing per xylem unit area (Castagneri et al., 2017). For the calculation of Ks, we first calculated the average theoretical hydraulic conductivity (Kh_t , kg m⁻¹ s⁻¹ MPa⁻¹), representing the amount of water flowing through the average tracheid for the ring t, according to the Hagen Poiseuille's law (Tyree and Zimmermann, 2002):

$$Kh_{t} = \frac{\left(\pi\rho/128\eta\right)\sum_{i=1}^{n}\left(LD_{i}^{4}\right)}{n}$$

where ρ is the density of water (998.2 kg m⁻³ at 20 °C), η is water viscosity (1.002 × 10⁻⁹ MPa s at 20 °C), LD is the radial lumen diameter of i^{th} tracheid, and n is the total number of measured tracheids for the ring

t. Xylem specific hydraulic conductivity ($Ks_b~{\rm kg~m^{-1}~s^{-1}~MPa^{-1}})$ was consequently calculated as:

$$Ks_t = Kh_t \times Dens_t$$

where $Dens_t$ is the cell density (number of cells per mm²) of the t^{th} ring. It should be noted that Ks can be calculated either 1) by dividing the total conductivity of all cells in the measured area of the ring by the measured area; or 2) by calculating the average theoretical conductivity for each cell in the measured area and multiplying for the cell density. Here we have chosen the second approach (as it can be seen in the formula, the numerator is the sum of theoretical conductivities of all cells in the ring), but the two approaches lead to identical results. In general, estimates of xylem theoretical hydraulic conductivity are generally expected to be lower than empirical measurements: however theoretical and empirical measurements of hydraulic conductivity are highly correlated, and theoretical proxies can be used for comparing stem conductivity between individuals (Steppe and Lemeur, 2007). In addition, to evaluate how xylem specific conductivity scaled up at the whole tree level, we calculated the total theoretical conductivity for each ring (*Kr*, kg m⁻¹ s⁻¹ MPa^{-1}) as:

$$Kr_t = Ks_t \times BAI_t$$

However, since by formulation Kr depends on BAI, this parameter could not be used as a proxy for hydraulic efficiency and was not used to test the relationships between xylem architecture and tree growth.

Xylem hydraulic safety was estimated by the cell wall reinforcement (*wrein*) (Hacke et al., 2001), considered a good proxy for xylem resistance to embolism and cell wall implosion (Guérin et al., 2020; Hereş et al., 2014). *wrein* ($\mu m/\mu m$)² was calculated for each ring as the squared ratio between the average cell wall thickness and the average lumen diameter, as follows:

$$wrein = \left(\frac{CWT}{LD}\right)^2$$

All anatomical (i.e. LD, CWT, *Dens*; Supplementary Figure 1) and hydraulic parameters (i.e. *Ks*, *Kr*, *wrein*) were averaged by ring, resulting in two datasets formed by 570 rings for *P. flexilis* and 635 for *P. longaeva*. The scaling of anatomical and hydraulic parameters along the stem was investigated considering only the last five rings (2009–2013), to 1) be sure to include only rings in the sapwood, and 2) to account for the vertical growth of the stem (i.e. at the time of formation of the inner rings in a microcore, that ring might have been located at a different distance from the stem apex). We tested several kinds of functions (i.e., power, exponential, linear) to describe the vertical scaling of anatomical and hydraulic parameters, selecting the one with the best fit according to the highest R².

2.4. Data analysis

The relationship between tree hydraulic parameters and climate was investigated using a dendroclimatic approach to assess short-term responses to recent climatic patterns. First, two mean annual chronologies of hydraulic parameter Ks and wrein were developed for P. flexilis and P. longaeva, covering the common period 1990-2013. Each chronology included all cores sampled at all heights along the stem, hence providing an exhaustive characterization of the interannual variability of hydraulic parameters at the whole tree level. The short length of the series and the lack of an objective criterion supported by scientific literature to determine the best approach for detrending such unusual proxies, led us to the decision to not standardize the chronologies, in order to preserve any signal driven by recent climatic trends. Partial correlation analyses were then run between raw chronologies of hydraulic proxies and daily time series of Tmax, Tmin, Ppt, VPDmin, and VPDmax over the period 1990–2013 using the package dendro Tools (Jevšenak and Levanič, 2018) for the R statistical environment (R Core Team, 2021). Partial correlations allow to quantify linear relationships between two variables while holding constant a third one (Jevšenak, 2020). When testing the relationship between hydraulic proxies, temperature, and VPD, precipitation was used as control variable, while to test the relationship between *Ks*, *wrein*, and Ppt, all the other climatic parameters were alternatively used as control variables. We checked partial correlations on running daily intervals with a minimum length of 14 days up to a maximum of 180 days, starting from January 1st to December 31st. In order to establish confidence intervals for each partial correlation coefficient, 500 bootstrap replications were run for each temporal window tested (Efron and Tibshirami, 1993).

To assess the relationships between hydraulic parameters and basal area increment, we produced several linear mixed models to test the effect of Ks and wrein on BAI and to what extent such relationship remains stable across stems (TREE) and under different climatic stress (DROUGHT). To define classes of drought, we ranked years from 1990 to 2013 according to values of summer (June to September) Standardized Precipitation Evapotranspiration Index (SPEI) (Vicente-Serrano et al., 2010) obtained from the global SPEI database (Beguería et al., 2014). The two sites fell within the same grid so that a single value could be determined for both sites. The average summer SPEI for the period $1990-2013 \text{ was } -0.126 \pm 0.557 \text{ (Supplementary Figure 2)}$. Each year was categorized according to five classes of SPEI, calculated as standard deviations (SD) from the 1990–2013 mean: very dry (SPEI < -1 SD from the mean); dry (-1 SD < SPEI < -0.5 SD from the mean); neutral (-0.5 SD < SPEI < +0.5 SD around the mean); wet (+0.5 SD < SPEI <+1 SD above the mean); *very wet* (SPEI > +1 SD above the mean).

The datasets of BAI, Ks, and wrein calculated for P. flexilis and P. longaeva were log-transformed (natural log) to correct their skewness. To account for a possible effect of previous years' Ks and wrein on current year's BAI, we calculated the average values of Ks and wrein up to five years prior to the current one (i.e. Ks_{1-2} being the average between current and previous year's Ks) and tested all of them as predictors (fixed effects). For each hydraulic parameter and species, using TREE and DROUGHT as random factors, we tested the accuracy of models with or without random slopes, to evaluate the effect of each random factor on the relationship between BAI and hydraulic parameters. The best model fit was determined by likelihood-ratio test, comparing a set of reduced models with the full one, alternatively omitting the random factor of interest (leave-one-out validation), until no further reduction of AIC value was observed. All analyses were performed using the R (R Core Team, 2021) package lme4 (Bates et al., 2015).

3. Results

3.1. Height-related variability of wood anatomical traits and hydraulic parameters

The variation of anatomical and hydraulic parameters measured along the stems could be described in most cases by a power function and only occasionally by other kinds of functions (e.g., exponential and linear; Table 1). In *P. flexilis*, radial lumen diameter (LD) scaled according to an exponential factor of 0.11, while in *P. longaeva* the scaling factor was 0.19 (Fig. 2a, Table 1). For stem lengths measured in both

species (3.75 – 7.25 m), *P. flexilis* showed larger tracheids (LD = 20.2 \pm 3.4 μm) and slightly narrower walls (CWT = 4.2 \pm 1.0 μm) than *P. longaeva* (LD = 18.8 \pm 2.1 μm ; CWT = 4.8 \pm 1.3 μm), while the modeled conduit size increased by + 8% for *P. flexilis* and + 14% for *P. longaeva*. In *P. flexilis*, cell wall thickness (CWT) increased linearly with stem length (Fig. 2b), resulting in a 10% increase in CWT along the common stem length. In *P. longaeva* an opposite trend was observed, with CWT decreasing exponentially along the stem, with thicker cells closer to the stem apex (5.1 μm at a stem length of 3.75 m) compared to the lower part of the stem (4.6 μm at 7.25 m; –9%; Fig. 2b). The number of cells per unit area (*Dens*) for both species was higher near the stem apex and decreased along the stem following a power function (Supplementary Figure 3), but *P. longaeva* showed on average a higher density of cells (1577 \pm 254 cells mm $^{-2}$) than *P. flexilis* (1441 \pm 300 cells mm $^{-2}$) in the common stem length.

The variation of xylem anatomy along the stem produced large effects on tree hydraulic parameters. Although xylem specific conductivity Ks scaled in both species according to a power function (Table 1), the increase in Ks between 3.75 and 7.25 m from the stem apex was + 37% in P. flexilis, while it was + 69% in P. longaeva (Fig. 2c). In P. longaeva, wrein increased upward by 31%, while in P. flexilis wrein increased slightly (+4%; Fig. 2d) in the opposite direction. The relationship between Ks and wrein highlighted a trade-off between hydraulic efficiency vs. safety (Supplementary Figure 4), in general more pronounced in P. longaeva than in P. flexilis. However, in P. flexilis Ks was mostly related to current-year wrein, while in P. longaeva the interannual variability of Ks was better described by the average wrein over the previous 5 years ($wrein_{1-5}$; Supplementary Figure 4).

In both species the vertical distribution of BAI was best fit by an exponential function (Table 1), although higher BAI values were observed in the common stem length in *P. longaeva* compared to *P. flexilis* (Fig. 3a). However, thanks to the different scaling of *Ks* along the stem, the total ring theoretical conductivity *Kr* varied almost identically in both *P. longaeva* and *P. flexilis* (Fig. 3b), following a power function with similar scaling factors (1.63 in *P. flexilis* and 1.53 in *P. longaeva*) and coefficients (232.5 in *P. flexilis* and 312.7 in *P. longaeva*; Table 1).

3.2. Temporal trends of hydraulic parameters and climate-hydraulic relationships

Average BAI was higher in *P. longaeva* (690 \pm 79 mm² yr $^{-1}$) than in *P. flexilis* (303 \pm 84 mm² yr $^{-1}$). In the period 1990–2013, annual basal area increment varied little, although in *P. longaeva* a non-significant (Mann-Kendall test p=0.36) decreasing trend was observed, contrary to the increasing, non-significant trend shown by *P. flexilis* (p=0.13; Fig. 4a). The mean annual *Ks* was slightly higher in *P. flexilis* (12.4e $^{-24}$ \pm 1.9e $^{-24}$ kg m $^{-1}$ s $^{-1}$ MPa $^{-1}$) than in *P. longaeva* (11.7e $^{-24}$ \pm 2.1e $^{-24}$ kg m $^{-1}$ s $^{-1}$ MPa $^{-1}$), with both species showing a significant (p<0.01 in *P. flexilis* and p<0.05 in *P. longaeva*) decrease in xylem specific conductivity between 1990 and 2013 ($-0.149e^{-24}$ and $-0.165e^{-24}$ kg m $^{-1}$ s $^{-1}$ MPa $^{-1}$ respectively in *P. flexilis* and *P. longaeva*; Fig. 4b). Average *wrein* was identical between the two species (0.054 ± 0.008 (µm/µm) 2 in *P. flexilis* and 0.054 ± 0.01 (µm/µm) 2 in *P. longaeva*), but *P. longaeva*

Table 1Formulas defining the variation of wood anatomical, hydraulic, and growth (BAI) parameters as a function of stem length (SL) in *Pinus flexilis* and *Pinus longaeva*.

Pinus flexilis						
Parameter Formula R ²	LD $\sim 16.61 * SL^{0.11}$ 0.286	CWT $\sim 0.115 * SL + 3.579$ 0.196	Ks $\sim 5.34e^{-24} * SL^{0.48}$ 0.690	<i>wrein</i> $\sim 0.04 * SL^{0.06}$ 0.002	BAI $\sim 61.95 * e^{(0.274*SL)}$ 0.771	Kr $\sim 232.5e^{-24} * SL^{1.63}$ 0.762
Pinus longaeva						
Parameter Formula R ²	LD $\sim 13.32 * SL^{0.19}$ 0.293	CWT $\sim 5.63 * e^{(-0.027*SL)}$ 0.192	Ks $\sim 2.10e^{-24} * SL^{0.80}$ 0.493	wrein $\sim 0.13*e^{(-0.105*SL)}$ 0.339	BAI $\sim 295.86 * e^{(0.099*SL)}$ 0.506	Kr $\sim 312.7e^{-24} * SL^{1.53}$ 0.743

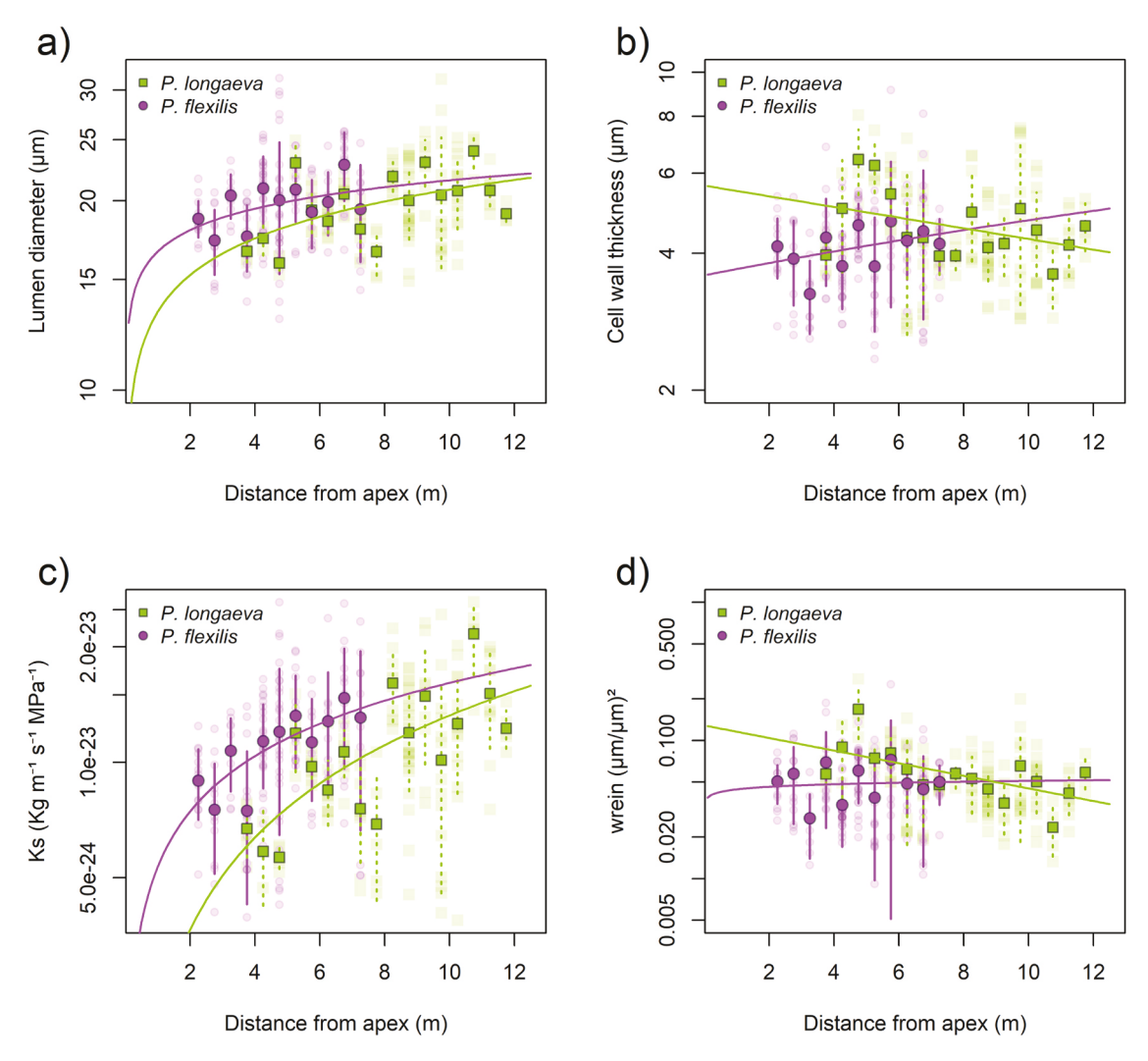


Fig. 2. Variation of xylem anatomy and hydraulic parameters along the stem for *Pinus flexilis* (purple circles) and *P. longaeva* (green squares): a) lumen diameter, b) cell wall thickness, c) xylem specific conductivity (Ks), and d) cell wall reinforcement (wrein). Light symbols are individual tree rings for the period 2009–2013, solid symbols are mean \pm 1 standard deviation for each height class (see text for details). Lines are functions interpolated to the mean values for each height class (see Table 1 for details).

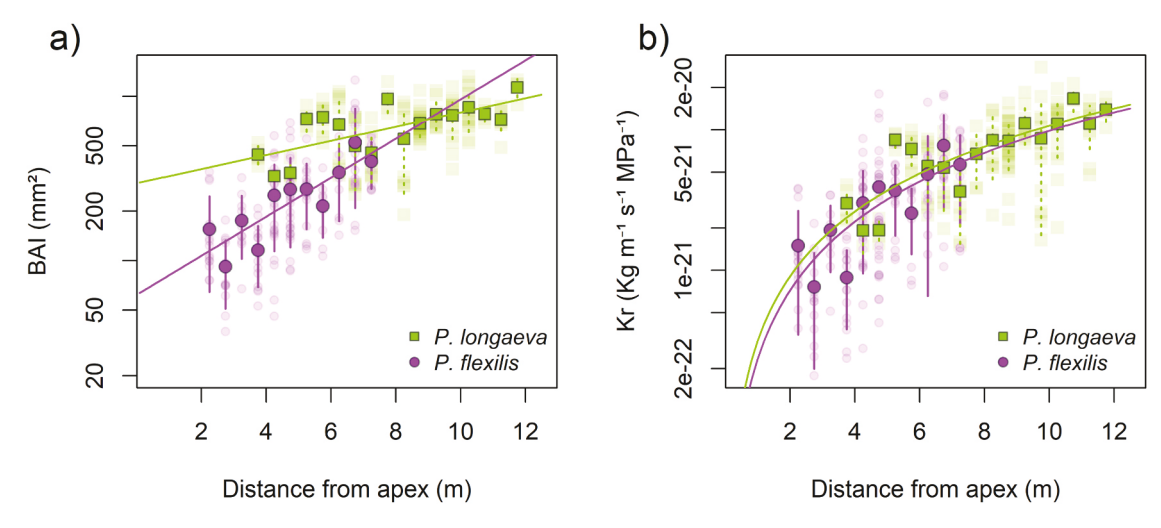


Fig. 3. Variation of BAI (a) and Kr (b) along the stem for *Pinus flexilis* (purple circles) and *P. longaeva* (green squares). Light symbols are individual tree rings for the period 2009–2013, solid symbols are mean ± 1 standard deviation for each height class (see text for details). Lines are functions interpolated to the mean values for each height class (see Table 1 for details).

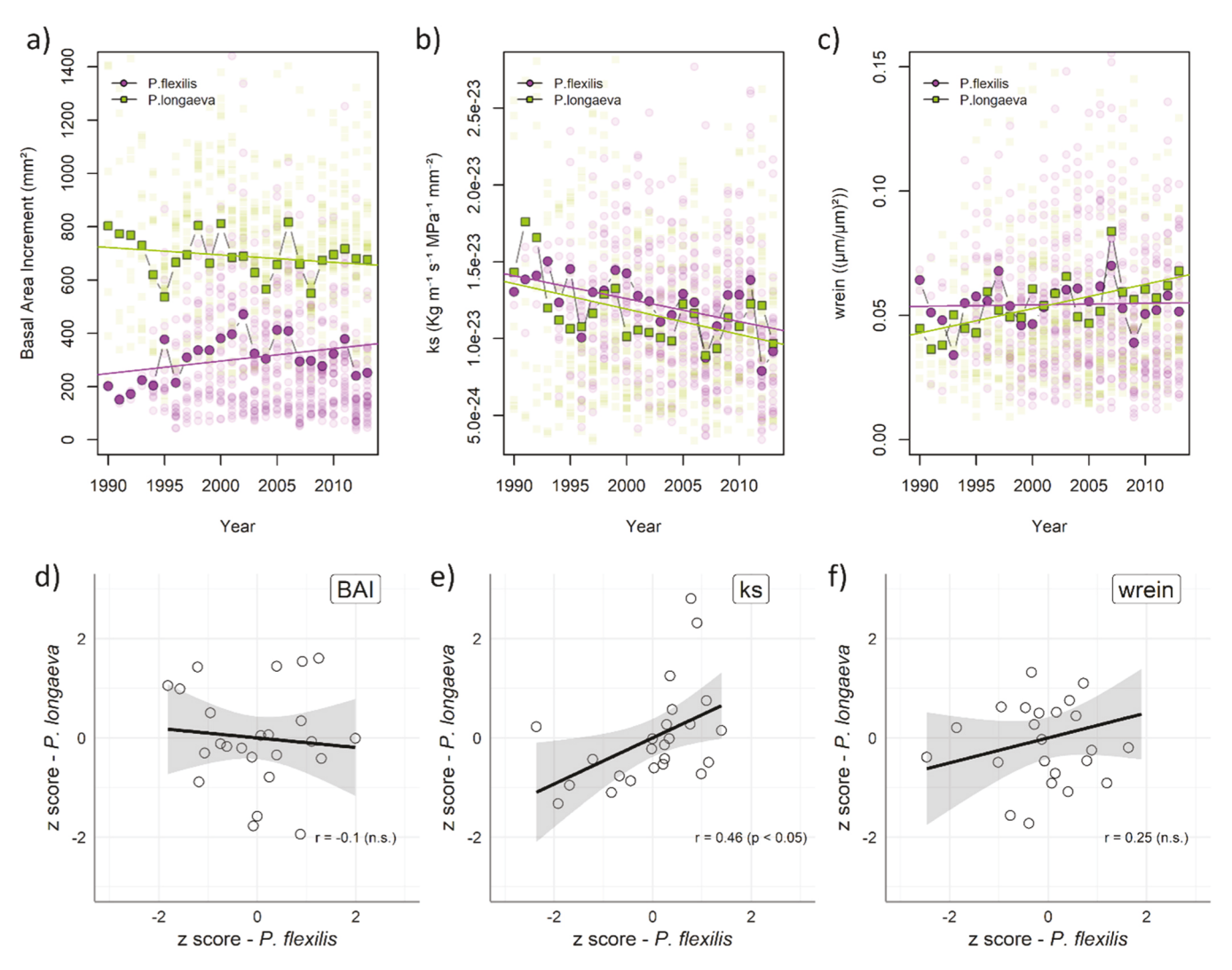


Fig. 4. Mean annual chronologies of a) basal area increment, b) xylem specific conductivity, and c) cell wall reinforcement from 1990 to 2013 for *Pinus flexilis* (purple circles and purple line) and *Pinus longaeva* (green squares and green line) (upper panels). Shaded symbols are individual tree rings. Correlations between normalized time-series of d) basal area increment, e) xylem specific conductivity, and f) cell wall reinforcement of *P. flexilis* and *P. longaeva* are shown for the same time period (1990 – 2013) in the lower panels.

presented an increase (p < 0.001) in *wrein* during 1990–2013 which was not observed in *P. flexilis* (Fig. 4c). Mean annual time-series of BAI and *wrein* were not or only slightly correlated between species (Fig. 4d, f), while series of *Ks* showed a significant correlation (r = 0.46, p < 0.05; Fig. 4e) between *P. flexilis* and *P. longaeva*.

In both species, xylem specific conductivity was negatively linked with Tmin, though at different temporal windows. *P. longaeva* correlated with Tmin (r=-0.63) over an 84-day period between June 26 and September 17 (Fig. 5a), and *P. flexilis* showed a stronger relationship (r=-0.76) over a 102-day timespan, from June 4 to September 13 (Fig. 5c). Cell wall reinforcement was also related to Tmin in *P. longaeva* (r=0.76), but such relationship emerged in the late summer, in a 55-days period between July 22 and September 14 (Fig. 5b). In *P. flexilis*, on the other hand, cell wall reinforcement was correlated during the early growing season, and over a shorter interval (20 days, from June 9 to June 28) with VPDmin (r=0.77) (Fig. 5d).

3.3. Effects of hydraulic parameters on basal area increment

Correlation analysis revealed that in *P. flexilis*, BAI was correlated with the average Ks over the last three years (Ks_{1-3}) (Pearson's correlation coefficient r = 0.56, p < 0.001), and with average wrein over the previous three years ($wrein_{1-3}$) (r = -0.18, p < 0.001). In *P. longaeva*,

on the other hand, BAI best correlated with current year Ks (r=0.37, p<0.001) and with the average wrein in the previous five years ($wrein_{1-5}$; r=-0.13, p<0.01). In both species, BAI was best predicted by a model including only TREE as random factor, but not DROUGHT (Table 2). Significant random intercepts and slopes emerged for Ks but not for wrein, indicating that the relationship $BAI \sim Ks$ was different between individuals, but not between levels of drought stress (Table 2, Fig. 6, Supplementary Figure 5). Ks had the highest model coefficients in both species, producing a positive effect on BAI, but in P. flexilis such relationship was more pronounced than in P. longaeva (Table 1). Even wrein had a slightly positive impact on tree basal area growth, greater in P. longaeva than in P. flexilis.

4. Discussion

4.1. Vertical variability of xylem hydraulic architecture

In *P. longaeva* and *P. flexilis*, lumen diameter widened from the top of the tree to the ground following a power function, which is the tip-to-base pattern observed across all phylogenetic plant groups and terrestrial biomes (Olson et al., 2021). Both species showed a scaling factor between 0.1 and 0.3, in agreement with experimental measurements in several angiosperms and conifer species (Anfodillo et al., 2006;

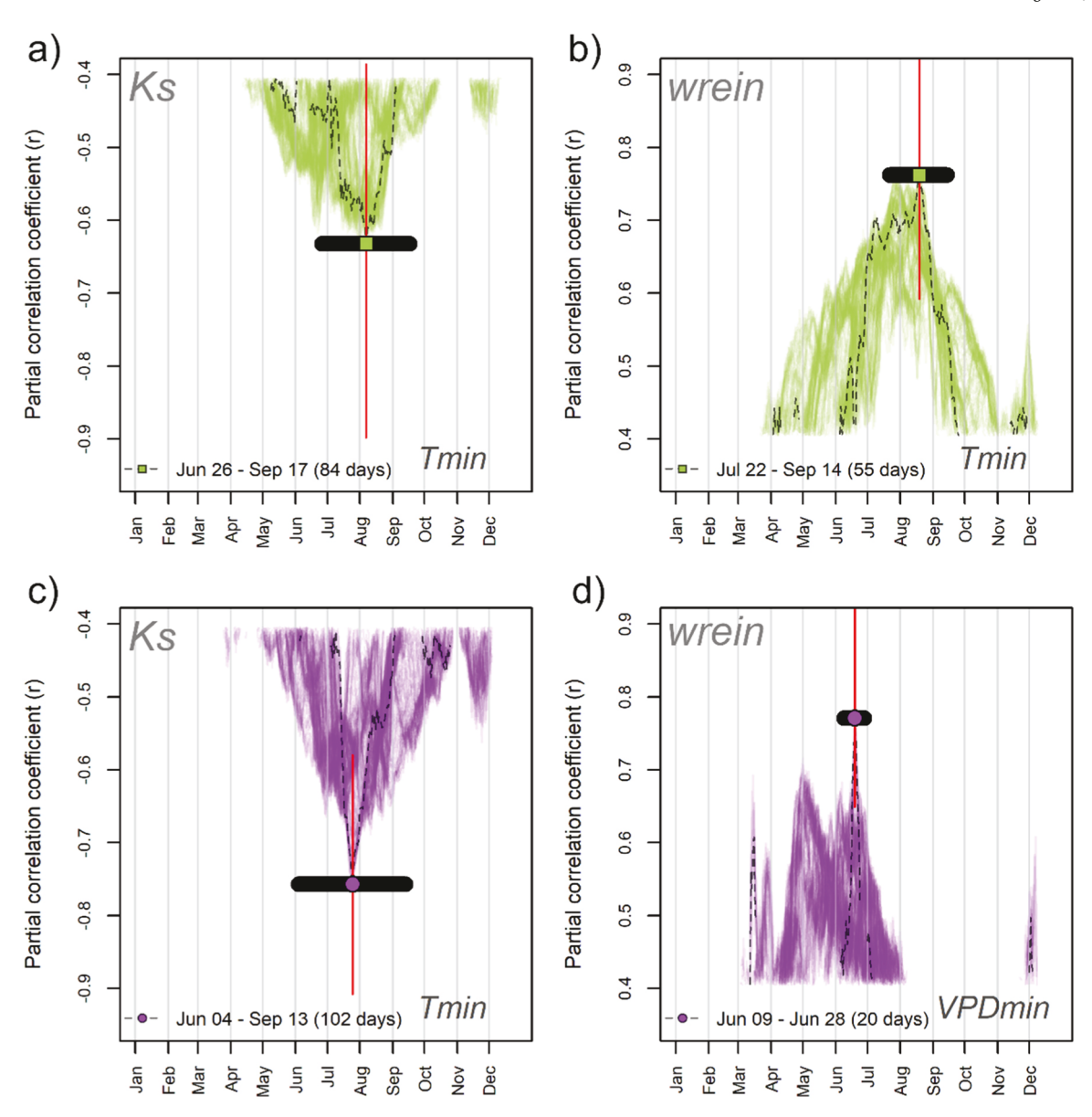


Fig. 5. Partial correlations between Ks (a,c) and wrein (b,d) in Pinus longaeva (green squares, top panels) and Pinus flexilis (purple circles, bottom panels) for the period 1990–2013. Each thin line represents a significant partial correlations with the climatic parameter listed in the bottom right corner, calculated for different temporal windows (see text for details). Dashed lines represent the temporal window with the highest partial correlation coefficient. Thick black horizontal lines highlight the extension of the temporal window with the highest partial correlation coefficient. Red vertical lines are 95% confidence intervals.

Anfodillo et al., 2012; Lazzarin et al., 2016; Petit et al., 2011; Rosell et al., 2017; Soriano et al., 2020). The higher scaling factor in P. longaeva (0.19) indicates a faster increase in lumen diameter with increasing distance from the apex, implying that this species minimizes the accumulation of path-length hydraulic resistance while maximizing hydraulic efficiency (Prendin et al., 2018), at the expense of specific conductivity (i.e. see the lower Ks of P. longaeva compared to P. flexilis in the common stem length) and height growth (Rosell et al., 2017). On the other hand, the lower scaling factor in P. flexilis (0.11) denotes a slower tip-to-base widening of tracheids diameter. Such behavior would allow P. flexilis to concentrate higher resistance at the apical part of the hydraulic path and then accumulate more path-length hydraulic resistance along the stem (Lechthaler et al., 2020), but it would also expose it to a higher risk of hydraulic failure due to the formation of embolisms and to higher carbon costs associated to the assemblage of fast widening conduits (Olson et al., 2018).

We did not find a clear height trend in cell wall thickness, consistently to what was reported for other conifer species (Anfodillo et al.,

2012). However, we found a difference between *P. flexilis*, showing a slight linear increase in CWT from the stem tip to the ground, and *P. longaeva*, in which CWT increased toward the top of the stem. Such pattern implies that in *P. flexilis* we should expect thicker cell walls at the stem base as the tree gets taller, while the thicker walls in the proximity of stem apex in *P. longaeva* lead to higher *wrein* values, contributing to higher margins of hydraulic safety. Increasing resistance to cell wall implosion close to the stem apex has also been observed in large individuals of *Pinus ponderosa* and *Pseudotsuga menziesii* (Domec et al., 2009). It should be noted that, despite the different scaling patterns of wood anatomical (LD and CWT) and hydraulic parameters (*Ks* and *wrein*) between *P. flexilis* and *P. longaeva*, the different scaling of BAI resulted in almost identical vertical patterns of total ring conductivity (*Kr*). This suggests convergent dynamics of hydraulic functioning based on the regulation of different xylem anatomical parameters.

The vertical variability of hydraulic parameters in *P. longaeva* defies the expected age- and size-related ontogenetic increase of conduit size (Carrer et al., 2015). In fact, despite a similar relationship between stem

Table 2 Summary of the best linear mixed models describing the relationship between BAI, xylem specific conductivity (*Ks*), and cell wall reinforcement (*wrein*) in *Pinus flexilis* and *Pinus longaeva*. For fixed terms, estimates and 95% confidence intervals (CI) are provided. Significance of random effects was calculated by likelihood-ratio test for models with/without each effect (leave-one-out verification).

	Pinus flexilis					
Response variable	log[BAI]					
Predictors	Estimates	CI	p			
Fixed Effects						
(Intercept)	70.14	60.69 - 79.58	< 0.001			
$log[Ks_{1-3}]$	1.20	1.02 - 1.38	< 0.001			
$log[wrein_{1-3}]$	0.37	0.27 - 0.47	< 0.001			
Random Effects	Variance	Std. Dev.				
$TREE_{Intercept}$	0.32	0.56				
$log[Ks_{1-3}] \mid TREE_{Slope}$	0.00	0.02				
Residual (σ²)	0.14					
Marginal R ²	0.24					
Conditional R ²	0.71					
	Pinus longaeva					
Response variable	log[BAI]					
Predictors	Estimates	CI	p			
Fixed Effects						
(Intercept)	15.48	10.76 - 20.20	< 0.001			
log[Ks]	0.16	0.08 - 0.25	< 0.01			
$log[wrein_{1-5}]$	0.12	0.05 - 0.19	0.001			
Random Effects	Variance	Std. Dev.				
$TREE_{Intercept}$	0.14	0.37				
log[Ks] TREE _{Slope}	0.00	0.00				
Residual (σ²)	0.08					
Marginal R ²	0.02					
Conditional R ²	0.58					

length and diameter in both species, with larger (and older) individuals of P. longaeva in the common stem length range 3.75 - 7.25 m (Supplementary Figure 6), average tracheid lumen diameter was smaller compared to P. flexilis. This was caused by the higher number of tracheids per mm² in P. longaeva, a peculiarity in its hydraulic architecture suggesting that the trade-off between hydraulic efficiency and safety in this species might be partially controlled by a strategy of space occupation (Savage et al., 2010). Such "packing rule" strategy acts on the number of conduits to modulate the trade-off between efficiency and safety (Sperry et al., 2008). In this case, the hydraulic architecture of P. longaeva would depend on a more complex set of interactions between mechanical constraints, which are expected to act on the wall-to-span ratio (Pittermann et al., 2006) and environmental constraints, particularly with the need to prevent both drought- and freeze-induced embolisms by adjusting tracheid lumen size (Carvalho et al., 2015; Pittermann and Sperry, 2006; Zheng et al., 2022).

4.2. Climatic drivers of interannual variability in xylem hydraulic parameters

Partial correlation results showed that, in both species, xylem hydraulic parameters were mostly coupled with air minimum temperature (Tmin), with both *Ks* and *wrein* showing a stronger climatic sensitivity in *P. flexilis*. The longer temporal window of climatic sensitivity for *Ks* than for *wrein* indicates that xylem hydraulic efficiency is modulated by climatic conditions recorded over a longer portion of the growing season compared to hydraulic safety. June appeared as a critical month for both hydraulic efficiency and safety in both species. Previous studies on xylogenesis conducted at these locations have revealed how the maximum cell division rate occurs in the last week of June (June 26) for *P. longaeva* (Ziaco et al., 2016b) and in the first one (June 8) for *P. flexilis* (Ziaco and Biondi, 2016), close to the summer solstice (Cabon et al., 2020b; Rossi et al., 2006b). Interestingly, these dates define also the beginning of the climatic window of maximum climatic sensitivity for *Ks* (in *P. longaeva*) and *wrein* (in *P. flexilis*), suggesting that the assemblage

of xylem hydraulic architecture occurs after the initial pulse of radial growth characterized by active cellular division and enlargement (Deslauriers et al., 2017), when cell wall deposition becomes the predominant process (Cuny et al., 2019; Cuny et al., 2015). Furthermore, transpiration rates peak in mid- to late-June in both species, suggesting an ample supply of carbohydrates sustaining maximum rate of xylem formation (Liu and Biondi, 2020).

In both species, the climatic response of Ks and wrein was linked to parameters (Tmin and VPDmin) defining evapotranspiration demands, rather than directly to water availability. The lack of a significant relationships between Ks and precipitation is particularly interesting, considering that LD, one of the main parameters contributing to the calculation of Ks, generally show a strong association with moisture conditions in arid environments (Balanzategui et al., 2021; Carvalho et al., 2015). This means that interannual variability of xylem hydraulic proxies can be decoupled from the climatic signal recorded in wood anatomical parameters. Less surprising is the lack of a precipitation signal in wrein, since CWT, the main driver of resistance to cell implosion, carries a weak climatic signal in water limited environments of the western US (Ziaco et al., 2016a). On the other hand, temperature is one of the main drivers of plant transpiration rates and the strong relationships between xylem hydraulics (i.e. Ks and wrein) and minimum temperature supports a recent long-term study, based on sub-hourly dendrometer records, showing the predominant control of evapotranspiration conditions on stem radial growth (Zweifel et al., 2021).

In the period 1990-2013 hydraulic efficiency decreased in both species. Considering that at both sites stand density is low, we can exclude changes in access to resources as a cause for such reduction in Ks, as confirmed by the lack of significant trends in BAI, but rather hypothesize a climatic control over this process. This is suggested by the significant correlation between annual time series of Ks of P. flexilis and P. longaeva, which points to the presence of a common climatic driver behind the interannual variability of xylem hydraulic efficiency, and it is further supported by the dendroclimatic analysis. Between 1990 and 2013, Tmin showed a +0.09 °C yr⁻¹ at the subalpine site and + 0.06 $^{\circ}$ C yr $^{-1}$ at the montane one, without any significant change in precipitation (Fig. 1b). When looking specifically at the temporal windows with maximum climatic sensitivity for Ks in P. longaeva (26 Jun -17 Sep) (Supplementary Figure 7a,b) and P. flexilis (4 Jun – 13 Sep) (Supplementary Figure 7c,d), the annual increase in Tmin was even higher (+0.15 °C and +0.11 °C per year respectively at the subalpine and montane sites). Similarly, different trends in climatic variability between the subalpine and montane site are likely to explain the increase in cell wall reinforcement observed in P. longaeva but not in P. flexilis. In P. longaeva, wrein was in fact related to Tmin between July 22 and September 14, and in the period 1990-2013 an increasing trend was recorded for this parameter at the subalpine site (Supplementary Figure 7e,f), while VPDmin, responsible for interannual variability of wrein in P. flexilis, did not show any significant trend (Supplementary Figure 7 g,h).

Using raw instead of standardized data may have contributed to the emergence of the observed climate-anatomy relationships, and the presence of decadal trends, particularly in Tmin, might have partially overshadowed the effect of interannual climatic variability on xylem hydraulic traits. However, the decision to use raw data was deemed consistent with respect to the goal of this research and with the current understanding of detrending techniques and their applicability to nonring-width proxies. First, in this work we aimed at investigating how tree hydraulic parameters derived from xylem anatomy are responding to current environmental changes, including short-term climatic trends, rather than testing their potential as paleoclimatic proxies (i.e see Lopez-Saez et al., 2023). This allowed us to use xylem anatomical and hydraulic parameters as a diagnostic tool for tree functioning and trait plasticity under specific growing conditions (Borghetti et al., 2020) in a region highly exposed to climate warming (Sambuco et al., 2020). Second, the short length of the temporal series analyzed (<30 years), the

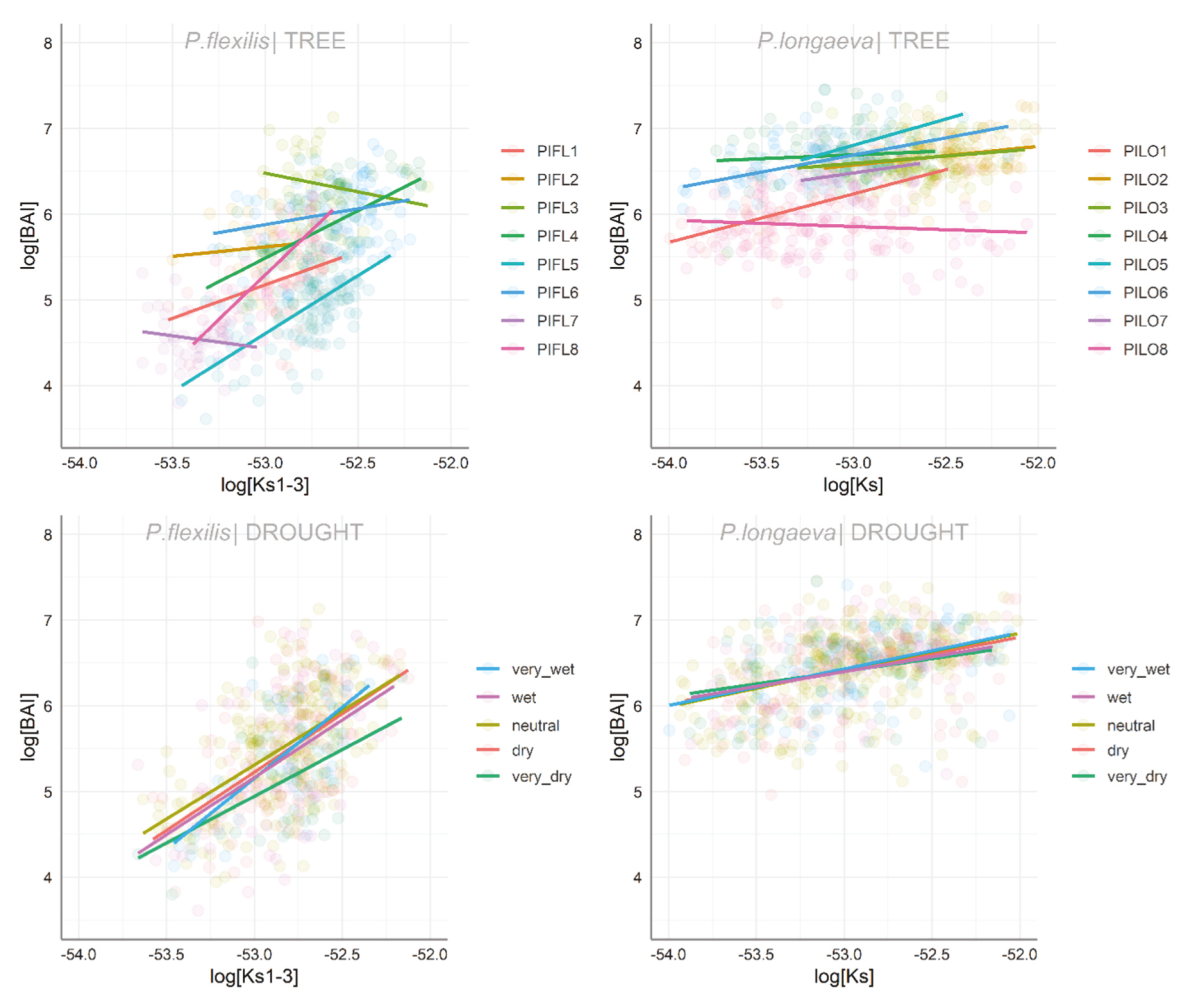


Fig. 6. Scatterplots showing the relationship between BAI and *Ks* for each random factor (TREE and DROUGHT) considered in this analysis. All random factors were plotted, regardless of their inclusion in the final models listed in Table 2. The linear mixed models are based on the full datasets (570 rings for *Pinus flexilis*; 635 for *Pinus longaeva*) measured in the period 1990–2013.

lack of commonly accepted criteria to determine the best standardization technique in time series of wood anatomical parameters (see Carrer et al., 2015), and the lack of information about ontogenetic trends for such proxies prevented us from performing a state-of-art standardization of time series of *Ks* and *wrein*. Finally, it should be noted that the usage of raw, undetrended series in quantitative wood anatomy is common practice, even with long time series (Carrer et al., 2018; Lopez-Saez et al., 2023).

4.3. Relationships between xylem hydraulic parameters and basal area increment

BAI was positively correlated with *Ks* in both species, but such relationships showed a large variability between trees. We found a species-specific temporal difference in the response of BAI to *Ks*, with the average *Ks* observed during the last three years being more correlated with current year's BAI in *P. flexilis* but not in *P. longaeva*. This means that the hydraulic adjustments in *P. longaeva* have a faster effect on the overall plant's growth, whereas in *P. flexilis*, changes in hydraulic architecture propagate over multiple years, potentially limiting its capacity to recover after a drought (Anderegg et al., 2015). Previous studies based on sap-flow sensors have highlighted a higher memory effect in *P. flexilis* compared to *P. longaeva* with respect to previous water conditions (Liu and Biondi, 2020). Cell wall reinforcement, on the other hand, emerged as a weak predictor for BAI in both species. In this case, BAI was linked with the 5-year average cell wall reinforcement in

P. longaeva, while it consistently remained correlated to the 3-year average in *P. flexilis*. Hence, in both species the mechanisms of hydraulic safety showed potentially higher legacy effects on tree growth than those for hydraulic efficiency.

In both species, the relationship between BAI and hydraulic parameters was largely affected by differences among individuals, as demonstrated by the difference between the marginal and conditional R² in all models. In particular, the significance of a random slope for Ks in each TREE level indicates that individuals of P. flexilis with higher BAI benefitted less from increasing xylem conductivity. At the same time a slightly positive effect of wrein on BAI emerged in both species, suggesting that investing in hydraulic safety could have positive effects on tree growth, despite higher building costs (Heres et al., 2014). Overall, in P. longaeva the relationship between stem hydraulic architecture and BAI did not significantly change during wet vs. dry years, possibly indicating a reduced climatic control on stem hydraulics. The weaker relationship between BAI and Ks, in light of the lower correlation between Ks and Tmin in P. longaeva compared to P. flexilis, is consistent with the low plasticity observed in interannual growth patterns (Smithers et al., 2021) and xylem anatomical features in P. longaeva (Connor and Lanner, 1990).

5. Conclusions

Our analysis of interannual variability of wood anatomical and hydraulic parameters at the whole-tree level allowed for better assessing

the influence of xylem functional traits on tree growth in two forests dominated by two of the most common species in the mountain ranges of the Great Basin of North America. First, our initial hypothesis of a differential control of hydraulic safety vs. efficiency on BAI in response to varying climatic conditions was not confirmed. While the temporal distribution of climatic sensitivity of parameters related to hydraulic efficiency and safety pointed toward a prioritization of safety in the more drought-exposed species, P. flexilis, xylem specific conductivity still exerted a stronger control on annual stem basal area increment in both species. Hence, we concluded that regardless of the strength of the efficiency vs. safety tradeoff at the xylem anatomical level, hydraulic conductivity can outcompete safety in determining stem growth even in water-limited environments. With specific regard to the Great Basin of North America, our data suggest that P. flexilis might be favored under warmer/wetter environmental conditions, thanks to its tighter control of Ks on BAI. On the other hand, P. longaeva might still prevail under warmer/drier climatic scenarios, thanks to its peculiar xylem hydraulic structure and relatively lower climatic sensitivity. Our study, conducted in natural conditions, is therefore consistent with the results of common garden experiments (Smithers et al., 2021), and highlights the need to include field-based observations of trait-growth relationships in vegetation models (Simeone et al., 2019). It also demonstrates the potential of functional traits derived from xylem anatomy as a diagnostic tool for forest ecosystem health and functioning and as a promising way to better understand climate-growth relationships and to forecast the species' growth plasticity in water-limited environments under future climate change scenarios.

CRediT authorship contribution statements

Emanuele Ziaco: Conceptualization, Methodology, Formal analysis, Investigation, Data curation, Visualization, Writing – original draft. **Xinsheng Liu:** Methodology, Formal analysis, Writing – review & editing. **Franco Biondi:** Conceptualization, Methodology, Formal analysis, Writing – review & editing, Funding acquisition. All authors approved the final version of this article.

Declaration of Competing Interest

The authors declare that they have no conflict of interest.

Data availability

Data will be made available on request.

Acknowledgements

E. Ziaco was funded by the US National Science Foundation (grant AGS-P2C2-1502379). F. Biondi was funded, in part, by the US National Science Foundation (grant AGS-P2C2-1903561). X. Liu was funded by the National Natural Science Foundation of China (grant 41961008).

The views and conclusions contained in this document are those of the authors and should not be interpreted as representing the opinions or policies of the funding agencies and supporting institutions. We thank two anonymous reviewers for the insightful comments and suggestions.

Appendix A. Supporting information

Supplementary data associated with this article can be found in the online version at doi:10.1016/j.dendro.2023.126116.

References

Anderegg, W., Meinzer, F., 2015, 2015. Wood Anatomy and Plant Hydraulics in a Changing Climate. In: Hacke, U. (Ed.), Functional and ecological xylem anatomy. Springer International Publishing, Switzerland, pp. 235–253. Chapter 9.

Anderegg, W.R.L., Klein, T., Bartlett, M., Sack, L., Pellegrini, A.F.A., Choat, B., Jansen, S., 2016. Meta-analysis reveals that hydraulic traits explain cross-species patterns of drought-induced tree mortality across the globe. Proc. Natl. Acad. Sci. 113, 5024 5020

- Anderegg, W.R.L., Schwalm, C., Biondi, F., Camarero, J.J., Koch, G., Litvak, M., Ogle, K., Shaw, J.D., Shevliakova, E., Williams, A.P., Wolf, A., Ziaco, E., Pacala, S., 2015. Pervasive drought legacies in forest ecosystems and their implications for carbon cycle models. Science 349, 528–532.
- Anfodillo, T., Carraro, V., Carrer, M., Fior, C., Rossi, S., 2006. Convergent tapering of xylem conduits in different woody species. New Phytol. 169, 279–290.
- Anfodillo, T., Deslauriers, A., Menardi, R., Tedoldi, L., Petit, G., Rossi, S., 2012. Widening of xylem conduits in a conifer tree depends on the longer time of cell expansion downwards along the stem. J. Exp. Bot. 63, 837–845.
- Balanzategui, D., Nordhauß, H., Heinrich, I., Biondi, F., Miley, N., Hurley, A.G., Ziaco, E., 2021. Wood anatomy of douglas-fir in eastern arizona and its relationship with pacific basin climate. Front. Plant Sci. 12.
- Bates, D., Mächler, M., Bolker, B., Walker, S., 2015. Fitting linear mixed-effects models using lme4. J. Stat. Softw. 67, 1–48.
- Beguería, S., Vicente-Serrano, S.M., Reig, F., Latorre, B., 2014. Standardized precipitation evapotranspiration index (SPEI) revisited: parameter fitting, evapotranspiration models, tools, datasets and drought monitoring. Int. J. Clim. 34, 3001–3023
- Berkelhammer, M., Still, C.J., Ritter, F., Winnick, M., Anderson, L., Carroll, R., Carbone, M., Williams, K.H., 2020. Persistence and plasticity in conifer water-use strategies. J. Geophys. Res. Biogeosciences 125 e2018JG004845.
- Biondi, F., Qeadan, F., 2008. A theory-driven approach to tree-ring standardization: defining the biological trend from expected basal area increment. Tree-Ring Res. 64 (81–96), 16.
- Borghetti, M., Gentilesca, T., Colangelo, M., Ripullone, F., Rita, A., 2020. Xylem functional traits as indicators of health in mediterranean forests. Curr. For. Rep. 6, 220–236.
- Bryukhanova, M., Fonti, P., 2013. Xylem plasticity allows rapid hydraulic adjustment to annual climatic variability. Trees 27, 485–496.
- Bunn, A.G., Salzer, M.W., Anchukaitis, K.J., Bruening, J.M., Hughes, M.K., 2018. Spatiotemporal variability in the climate growth response of high elevation bristlecone pine in the white mountains of California. Geophys Res Lett. 45, 13.312–313.321.
- Bunn, A.G., Korpela, M., Biondi, F., Campelo, F., Mérian, P., Mudelsee, M., Qeadan, F., Schulz, M., Zang, C., 2014. dplR: Dendrochronology Program Library in R, R package version 1.5.9 ed. (http://CRAN.R-project.org/package=dplR).
- Buttò, V., Rossi, S., Deslauriers, A., Morin, H., 2019. Is size an issue of time? relationship between the duration of xylem development and cell traits. Ann. Bot. 123, 1257–1265.
- Cabon, A., Peters, R.L., Fonti, P., Martínez-Vilalta, J., De Cáceres, M., 2020b. Temperature and water potential co-limit stem cambial activity along a steep elevational gradient. New Phytol. 226, 1325–1340.
- Cabon, A., Fernández-de-Uña, L., Gea-Izquierdo, G., Meinzer, F.C., Woodruff, D.R., Martínez-Vilalta, J., De Cáceres, M., 2020a. Water potential control of turgor-driven tracheid enlargement in Scots pine at its xeric distribution edge. New Phytol. 225, 209–221
- Carrer, M., Unterholzner, L., Castagneri, D., 2018. Wood anatomical traits highlight complex temperature influence on Pinus cembra at high elevation in the Eastern Alps. Int. J. Biometeorol. 62, 1745–1753.
- Carrer, M., von Arx, G., Castagneri, D., Petit, G., 2015. Distilling allometric and environmental information from time series of conduit size: the standardization issue and its relationship to tree hydraulic architecture. Tree Phys. 35, 27–33.
- Carvalho, A., Nabais, C., Vieira, J., Rossi, S., Campelo, F., 2015. Plastic response of tracheids in pinus pinaster in a water-limited environment: adjusting lumen size instead of wall thickness. PLoS One 10, e0136305.
- Castagneri, D., Regev, L., Boaretto, E., Carrer, M., 2017. Xylem anatomical traits reveal different strategies of two mediterranean oaks to cope with drought and warming. Environ. Exp. Bot. 133, 128–138.
- Chenlemuge, T., Schuldt, B., Dulamsuren, C., Hertel, D., Leuschner, C., Hauck, M., 2015. Stem increment and hydraulic architecture of a boreal conifer (Larix sibirica) under contrasting macroclimates. Trees 29, 623–636.
- Cochard, H., Pimont, F., Ruffault, J., Martin-StPaul, N., 2021. SurEau: a mechanistic model of plant water relations under extreme drought. Ann. Sci. 78, 55.
- Connor, K.F., Lanner, R.M., 1990. Effects of tree age on secondary xylem and phloem anatomy in stems of Great Basin bristlecone pine (Pinus longaeva). Am. J. Bot. 77, 1070–1077.
- Cook, B.I., Mankin, J.S., Marvel, K., Williams, A.P., Smerdon, J.E., Anchukaitis, K.J., 2020. Twenty-first century drought projections in the CMIP6 forcing scenarios. Earth'S. Future 8 e2019EF001461.
- Cruiziat, P., Cochard, H., Améglio, T., 2002. Hydraulic architecture of trees: main concepts and results. Ann. Sci. 59, 723–752.
- Cuny, H.E., Rathgeber, C.B.K., Frank, D., Fonti, P., Fournier, M., 2014. Kinetics of tracheid development explain conifer tree-ring structure. New Phytol. 203, 1231–1241.
- Cuny, H.E., Fonti, P., Rathgeber, C.B.K., von Arx, G., Peters, R.L., Frank, D.C., 2019.
 Couplings in cell differentiation kinetics mitigate air temperature influence on conifer wood anatomy. Plant Cell Environ. 42, 1222–1232.
- Cuny, H.E., Rathgeber, C.B.K., Frank, D., Fonti, P., Mäkinen, H., Prislan, P., Rossi, S., del Castillo, E.M., Campelo, F., Vavrčík, H., Camarero, J.J., Bryukhanova, M.V., Jyske, T., Gričar, J., Gryc, V., De Luis, M., Vieira, J., Čufar, K., Kirdyanov, A.V., Oberhuber, W., Treml, V., Huang, J.-G., Li, X., Swidrak, I., Deslauriers, A., Liang, E., Nöjd, P., Gruber, A., Nabais, C., Morin, H., Krause, C., King, G., Fournier, M., 2015.

- Woody biomass production lags stem-girth increase by over one month in coniferous forests. Nat. Plants 1, 15160.
- Daly, C., Halbleib, M., Smith, J.I., Gibson, W.P., Doggett, M.K., Taylor, G.H., Curtis, J., Pasteris, P.P., 2008. Physiographically sensitive mapping of climatological temperature and precipitation across the conterminous United States. Int. J. Climatol. 28, 2031–2064.
- De Micco, V., Aronne, G., Baas, P., 2008. Wood anatomy and hydraulic architecture of stems and twigs of some Mediterranean trees and shrubs along a mesic-xeric gradient. Trees 22, 643–655.
- Deslauriers, A., Fonti, P., Rossi, S., Rathgeber, C.B.K., Gričar, J., 2017. Ecophysiology and Plasticity of Wood and Phloem Formation. In: Amoroso, M.M., Daniels, L.D., Baker, P.J., Camarero, J.J. (Eds.), Dendroecology: Tree-Ring Analyses Applied to Ecological Studies. Springer International Publishing, Cham, pp. 13–33.
- Domec, J.C., Gartner, B.L., 2003. Relationship between growth rates and xylem hydraulic characteristics in young, mature and old-growth ponderosa pine trees. Plant Cell Environ. 26, 471–483.
- Domec, J.-C., Warren, J.M., Meinzer, F.C., Lachenbruch, B., 2009. Safety factors for Xylem failure by implosion and air-seeding within roots, trunks and branches of young and old conifer trees. IAWA J. 30, 101–120.
- Efron, B., Tibshirami, R., 1993. An Introduction to the Bootstrap. Chapman & Hall,, New York.
- Fan, Z.-X., Zhang, S.-B., Hao, G.-Y., Ferry Slik, J.W., Cao, K.-F., 2012. Hydraulic conductivity traits predict growth rates and adult stature of 40 Asian tropical tree species better than wood density. J. Ecol. 100, 732–741.
- Férriz, M., Martin-Benito, D., Fernández-de-Simón, M.B., Conde, M., García-Cervigón, A. I., Aranda, I., Gea-Izquierdo, G., 2023. Functional phenotypic plasticity mediated by water stress and [CO2] explains differences in drought tolerance of two phylogenetically close conifers. Tree Phys.
- Gleason, S.M., Stephens, A.E.A., Tozer, W.C., Blackman, C.J., Butler, D.W., Chang, Y., Cook, A.M., Cooke, J., Laws, C.A., Rosell, J.A., Stuart, S.A., Westoby, M., 2018. Shoot growth of woody trees and shrubs is predicted by maximum plant height and associated traits. Funct. Ecol. 32, 247–259.
- Gleason, S.M., Westoby, M., Jansen, S., Choat, B., Hacke, U.G., Pratt, R.B., Bhaskar, R., Brodribb, T.J., Bucci, S.J., Cao, K.-F., Cochard, H., Delzon, S., Domec, J.-C., Fan, Z.-X., Feild, T.S., Jacobsen, A.L., Johnson, D.M., Lens, F., Maherali, H., Martínez-Vilalta, J., Mayr, S., McCulloh, K.A., Mencuccini, M., Mitchell, P.J., Morris, H., Nardini, A., Pittermann, J., Plavcová, L., Schreiber, S.G., Sperry, J.S., Wright, I.J., Zanne, A.E., 2016. Weak tradeoff between xylem safety and xylem-specific hydraulic efficiency across the world's woody plant species. New Phytol. 209, 123–136.
- Grayson, D.K., 2011. The Great Basin. A Natural Prehistory, 1 ed..,. University of California Press..
- Guay, R., 2013. WinCELL 2013 for wood cell analysis. Regent Instruments Canada Inc., Ontario.
- Guérin, M., von Arx, G., Martin-Benito, D., Andreu-Hayles, L., Griffin, K.L., McDowell, N. G., Pockman, W., Gentine, P., 2020. Distinct xylem responses to acute vs prolonged drought in pine trees. Tree Phys. 40, 605–620.
- Hacke, U.G., Sperry, J.S., Pockman, W.T., Davis, S.D., McCulloh, K.A., 2001. Trends in wood density and structure are linked to prevention of xylem implosion by negative pressure. Oecologia 126, 457–461.
- Heres, A.-M., Camarero, J.J., López, B.C., Martínez-Vilalta, J., 2014. Declining hydraulic performances and low carbon investments in tree rings predate Scots pine drought-induced mortality. Trees 28, 1737–1750.
- Hoeber, S., Leuschner, C., Köhler, L., Arias-Aguilar, D., Schuldt, B., 2014. The importance of hydraulic conductivity and wood density to growth performance in eight tree species from a tropical semi-dry climate. Ecol. Manag. 330, 126–136.
- Hudson, P.J., Limousin, J.M., Krofcheck, D.J., Boutz, A.L., Pangle, R.E., Gehres, N., McDowell, N.G., Pockman, W.T., 2018. Impacts of long-term precipitation manipulation on hydraulic architecture and xylem anatomy of piñon and juniper in Southwest USA. Plant Cell Env 41, 421-435.
- Islam, M., Rahman, M., Bräuning, A., 2019. Long-term wood anatomical time series of two ecologically contrasting tropical tree species reveal differential hydraulic adjustment to climatic stress. Agric. For. Meteorol. 265, 412–423.
- Jevšenak, J., 2020. New features in the dendroTools R package: bootstrapped and partial correlation coefficients for monthly and daily climate data. Dendrochronologia 63, 125763
- Jevšenak, J., Levanič, T., 2018. dendroTools: R package for studying linear and nonlinear responses between tree-rings and daily environmental data. Dendrochronologia 48, 32–39
- Khansaritoreh, E., Schuldt, B., Dulamsuren, C., 2018. Hydraulic traits and tree-ring width in Larix sibirica Ledeb. as affected by summer drought and forest fragmentation in the Mongolian forest steppe. Ann. Sci. 75, 30.
- Lanner, R.M., 1984. Trees of the Great Basin: A Natural History. University of Nevada Press.
- Lazzarin, M., Crivellaro, A., Williams, C.B., Dawson, T.E., Mozzi, G., Anfodillo, T., 2016.
 Tracheid and pit anatomy vary in tandem in a tall Sequoiadendron giganteum tree.
 Iawa J. 37, 172–185.
- Lechthaler, S., Kiorapostolou, N., Pitacco, A., Anfodillo, T., Petit, G., 2020. The total path length hydraulic resistance according to known anatomical patterns: what is the shape of the root-to-leaf tension gradient along the plant longitudinal axis. J. Theor. Biol. 502, 110369.
- Liu, X., Biondi, F., 2020. Transpiration drivers of high-elevation five-needle pines (Pinus longaeva and Pinus flexilis) in sky-island ecosystems of the North American Great Basin. Sci. Total Environ. 739, 139861.
- Liu, X., Ziaco, E., Biondi, F., 2021. Water-use efficiency of co-occurring sky-island pine species in the North American Great Basin. Front Plant Sci. 12.

Lopez-Saez, J., Corona, C., von Arx, G., Fonti, P., Slamova, L., Stoffel, M., 2023. Tree-ring anatomy of Pinus cembra trees opens new avenues for climate reconstructions in the European Alps. Sci. Total Environ. 855, 158605.

- Lourenço, J., Houle, D., Duchesne, L., Kneeshaw, D., 2022. Interactions between xylem traits linked to hydraulics during xylem development optimize growth performance in conifer seedlings. bioRxiv, 2021.2012.2024.474017.
- McCulloh, K.A., Johnson, D.M., Meinzer, F.C., Woodruff, D.R., 2014. The dynamic pipeline: hydraulic capacitance and xylem hydraulic safety in four tall conifer species. Plant Cell Environ. 37, 1171–1183.
- Mencuccini, M., Grace, J., Fioravanti, M., 1997. Biomechanical and hydraulic determinants of tree structure in Scots pine: anatomical characteristics. Tree Phys. 17, 105–113.
- Mensing, S., Strachan, S., Arnone, J., Fenstermaker, L., Biondi, F., Devitt, D., Johnson, B., Bird, B., Fritzinger, E., 2013. A network for observing great basin climate change. Eos, Trans. Am. Geophys. Union 94, 105–106.
- Millar, C.I., Westfall, R.D., Delany, D.L., Flint, A.L., Flint, L.E., 2015. Recruitment patterns and growth of high-elevation pines in response to climatic variability (1883–2013), in the western Great Basin, USA. Can. J. Res 45, 1299–1312.
- Olson, M.E., Anfodillo, T., Gleason, S.M., McCulloh, K.A., 2021. Tip-to-base xylem conduit widening as an adaptation: causes, consequences, and empirical priorities. New Phytol. 229, 1877–1893.
- Olson, M.E., Soriano, D., Rosell, J.A., Anfodillo, T., Donoghue, M.J., Edwards, E.J., León-Gómez, C., Dawson, T., Camarero Martínez, J.J., Castorena, M., Echeverría, A., Espinosa, C.I., Fajardo, A., Gazol, A., Isnard, S., Lima, R.S., Marcati, C.R., Méndez-Alonzo, R., 2018. Plant height and hydraulic vulnerability to drought and cold. Proc. Natl. Acad. Sci. 115, 7551–7556
- Pacheco, A., Camarero, J.J., Carrer, M., 2015. Linking wood anatomy and xylogenesis allows pinpointing of climate and drought influences on growth of coexisting conifers in continental Mediterranean climate. Tree Phys. 36, 502–512.
- Pellizzari, E., Camarero, J.J., Gazol, A., Sangüesa-Barreda, G., Carrer, M., 2016. Wood anatomy and carbon-isotope discrimination support long-term hydraulic deterioration as a major cause of drought-induced dieback. Glob. Chang Biol. 22, 2125–2137.
- Petit, G., Anfodillo, T., Carraro, V., Grani, F., Carrer, M., 2011. Hydraulic constraints limit height growth in trees at high altitude. New Phytol. 189, 241–252.
- Pfautsch, S., 2016. Hydraulic anatomy and function of trees-basics and critical developments. Curr. For. Rep. 2, 236–248.
- Piermattei, A., von Arx, G., Avanzi, C., Fonti, P., Gärtner, H., Piotti, A., Urbinati, C., Vendramin, G.G., Büntgen, U., Crivellaro, A., 2020. Functional relationships of wood anatomical traits in Norway Spruce. Front. Plant Sci. 11.
- Pittermann, J., Sperry, J.S., 2006. Analysis of freeze-thaw embolism in conifers. the interaction between cavitation pressure and tracheid size. Plant Phys. 140, 374–382.
- Pittermann, J., Sperry, J.S., Wheeler, J.K., Hacke, U.G., Sikkema, E.H., 2006. Mechanical reinforcement of tracheids compromises the hydraulic efficiency of conifer xylem. Plant Cell Environ. 29, 1618–1628.
- Poorter, L., McDonald, I., Alarcón, A., Fichtler, E., Licona, J.-C., Peña-Claros, M., Sterck, F., Villegas, Z., Sass-Klaassen, U., 2010. The importance of wood traits and hydraulic conductance for the performance and life history strategies of 42 rainforest tree species. New Phytol. 185, 481–492.
- Prendin, A.L., Mayr, S., Beikircher, B., von Arx, G., Petit, G., 2018. Xylem anatomical adjustments prioritize hydraulic efficiency over safety as Norway spruce trees grow taller. Tree Phys. 38, 1088–1097.
- Puchi, P.F., Camarero, J.J., Battipaglia, G., Carrer, M., 2021. Retrospective analysis of wood anatomical traits and tree-ring isotopes suggests site-specific mechanisms triggering Araucaria araucana drought-induced dieback. Glob. Chang Biol. 27, 6394–6408.
- R Core Team, 2021. R: A language and environment for statistical computing. R Foundation for Statistical Computing, Vienna, Austria.
- Rosas, T., Mencuccini, M., Batlles, C., Regalado, Í., Saura-Mas, S., Sterck, F., Martínez-Vilalta, J., 2021. Are leaf, stem and hydraulic traits good predictors of individual tree growth. Funct. Ecol. 35, 2435–2447.
- Rosell, J.A., Olson, M.E., Anfodillo, T., 2017. Scaling of Xylem vessel diameter with plant size: causes, predictions, and outstanding questions. Curr. For. Rep. 3, 46–59.
- Rossi, S., Anfodillo, T., Menardi, R., 2006a. Trephor: a new tool for sampling microcores from tree stems. Iawa J. 27, 89–97.
- Rossi, S., Deslauriers, A., Anfodillo, T., Morin, H., Saracino, A., Motta, R., Borghetti, M., 2006b. Conifers in cold environments synchronize maximum growth rate of tree-ring formation with day length. New Phytol. 170, 301–310.
- Russo, S.E., Jenkins, K.L., Wiser, S.K., Uriarte, M., Duncan, R.P., Coomes, D.A., 2010. Interspecific relationships among growth, mortality and xylem traits of woody species from New Zealand. Funct. Ecol. 24, 253–262.
- Salzer, M.W., Larson, E.R., Bunn, A.G., Hughes, M.K., 2014. Changing climate response in near-treeline bristlecone pine with elevation and aspect. Environ. Res. Lett. 9, 114007.
- Sambuco, E.N., Mark, B.G., Patrick, N., DeGrand, J.Q., Porinchu, D.F., Reinemann, S.A., Baker, G.M., Box, J.E., 2020. Mountain temperature changes from embedded sensors spanning 2000 m in Great Basin National Park. 2006–2018. Front. Earth Sci. 8.
- Sasani, N., Paques, L.E., Boulanger, G., Singh, A.P., Gierlinger, N., Rosner, S., Brendel, O., 2021. Physiological and anatomical responses to drought stress differ between two larch species and their hybrid. Trees 35, 1467–1484.
- Savage, V.M., Bentley, L.P., Enquist, B.J., Sperry, J.S., Smith, D.D., Reich, P.B., von Allmen, E.I., 2010. Hydraulic trade-offs and space filling enable better predictions of vascular structure and function in plants. Proc. Natl. Acad. Sci. 107, 22722–22727.
- Simeone, C., Maneta, M.P., Holden, Z.A., Sapes, G., Sala, A., Dobrowski, S.Z., 2019. Coupled ecohydrology and plant hydraulics modeling predicts ponderosa pine

- seedling mortality and lower treeline in the US Northern Rocky Mountains. New Phytol. 221, 1814–1830.
- Smithers, B.V., Alongi, F., North, M.P., 2021. Live fast, die young: climate shifts may favor great basin bristlecone pine or limber pine in sub-alpine forest establishment. Ecol. Manag. 494, 119339.
- Smithers, B.V., North, M.P., Millar, C.I., Latimer, A.M., 2018. Leap frog in slow motion: divergent responses of tree species and life stages to climatic warming in Great Basin subalpine forests. Glob. Chang Biol. 24, e442–e457.
- Soriano, D., Echeverría, A., Anfodillo, T., Rosell, J.A., Olson, M.E., 2020. Hydraulic traits vary as the result of tip-to-base conduit widening in vascular plants. J. Exp. Bot. 71, 4232–4242.
- Sperry, J.S., Meinzer, F.C., McCulloh, K.A., 2008. Safety and efficiency conflicts in hydraulic architecture: scaling from tissues to trees. Plant Cell Environ. 31, 632–645.
- Steppe, K., Lemeur, R., 2007. Effects of ring-porous and diffuse-porous stem wood anatomy on the hydraulic parameters used in a water flow and storage model. Tree Phys. 27, 43–52.
- Sterck, F.J., Martínez-Vilalta, J., Mencuccini, M., Cochard, H., Gerrits, P., Zweifel, R., Herrero, A., Korhonen, J.F.J., Llorens, P., Nikinmaa, E., Nolè, A., Poyatos, R., Ripullone, F., Sass-Klaassen, U., 2012. Understanding trait interactions and their impacts on growth in Scots pine branches across Europe. Funct. Ecol. 26, 541–549.
- Stevenson, S., Coats, S., Touma, D., Cole, J., Lehner, F., Fasullo, J., Otto-Bliesner, B., 2022. Twenty-first century hydroclimate: a continually changing baseline, with more frequent extremes. Proc. Natl. Acad. Sci. 119, e2108124119.
- Stokes, M.A., Smiley, T.L., 1996. An Introduction to Tree-ring Dating. University of Arizona Press.
- Tyree, M.T., Zimmermann, M.H., 2002. Xylem Structure and the Ascent of Sap. Springer,, Berlin, Heidelberg.

- Vicente-Serrano, S.M., Beguería, S., López-Moreno, J.I., Angulo, M., El Kenawy, A., 2010.

 A New Global 0.5° Gridded Dataset (1901–2006) of a multiscalar drought index: comparison with current drought index datasets based on the palmer drought severity index. J. Hydrometeorol. 11, 1033–1043.
- Von Arx, G., Crivellaro, A., Prendin, A.L., Čufar, K., Carrer, M., 2016. Quantitative wood anatomy-practical guidelines. Front. Plant Sci. 7, 781.
- Vospernik, S., 2021. Basal area increment models accounting for climate and mixture for Austrian tree species. Ecol. Manag. 480, 118725.
- Zheng, J., Li, Y., Morris, H., Vandelook, F., Jansen, S., 2022. Variation in tracheid dimensions of conifer xylem reveals evidence of adaptation to environmental conditions. Front. Plant Sci. 13.
- Ziaco, E., Biondi, F., 2016. Tree growth, cambial phenology, and wood anatomy of limber pine at a Great Basin (USA) mountain observatory. Trees 30, 1507–1521.
- Ziaco, E., Biondi, F., 2018. Stem circadian phenology of four pine species in naturally contrasting climates from sky-island forests of the Western USA. Forests 9, 396.
- Ziaco, E., Biondi, F., Heinrich, I., 2016a. Wood cellular dendroclimatology: testing new proxies in Great Basin Bristlecone pine. Front. Plant Sci. 7, 1602.
- Ziaco, E., Biondi, F., Rossi, S., Deslauriers, A., 2016b. Environmental drivers of cambial phenology in Great Basin bristlecone pine. Tree Phys. 36, 818–831.
- Zimmermann, J., Link, R.M., Hauck, M., Leuschner, C., Schuldt, B., 2021. 60-year record of stem xylem anatomy and related hydraulic modification under increased summer drought in ring- and diffuse-porous temperate broad-leaved tree species. Trees 35, 919–937
- Zweifel, R., Sterck, F., Braun, S., Buchmann, N., Eugster, W., Gessler, A., Häni, M., Peters, R.L., Walthert, L., Wilhelm, M., Ziemińska, K., Etzold, S., 2021. Why trees grow at night. New Phytol. 231, 2174–2185.